Indian Journal of Pure & Applied Physics
Vol. 57, July 2019, pp. 498-505

Non-isothermal crystallization kinetics of chalcogenide $Se_{79}Te_{20}Pb_1$ glass using differential scanning calorimetry technique

Balbir Singh Patial[a,b*], Himani[c] & Nagesh Thakur[c]

[a]State Project Directorate, Rashtriya Uchchatar Shiksha Abhiyan (RUSA), Directorate of Higher Education, Shimla 171 001, India

[b]Department of Physics, Government College of Sunni, Shimla 171 301, India

[c]Department of Physics, H P University, Summer Hill, Shimla 171 005, India

Received 09 April 2017; accepted 29 April 2019

In the present paper, the overall amorphous-crystallization transformation kinetics of chalcogenide $Se_{79}Te_{20}Pb_1$ alloy has been reported using differential scanning calorimetry technique under non-isothermal conditions at three different heating rates (5, 10 and 15 °C/min). Amorphous nature of the investigated alloy is verified using X-ray diffraction. The glass transition region has been investigated using three empirical approaches and consonance of these methods has been discussed. The apparent activation energy for glass transition and crystallization region has been deduced using different methods. The Avrami exponent of the investigated alloy indicates one dimension growth of the investigated glass. The deduced values of Hruby's parameter and fragility index indicate that amorphous alloy has been formed from good glass forming liquids.

Keywords: Chalcogenide glass, DSC, Non-isotherma, Activation energy, Glass forming ability

1 Introduction

Chalcogenide amorphous materials have been captivated much attention during the last few years because of their interesting optical, electrical, dielectric, thermal and physical properties by changing the composition. Mostly Se based chalcogenide materials are preferred due to its commercial use and technological applications. Moreover, its device applications like switching, memory and xerography etc. made it attractive. Se based glassy alloys are very important material because of its application in reversible phase transformation most usually used in xerographic applications[1]. But pure Se has short life time and low sensitivity[2] although it is characterized by high viscosity. This problem can be overcome by alloying Se with some impurities such as Te which in terms gives high sensitivity, greater hardness, high crystallization temperature (T_p) and small ageing effects as compared to pure Se glass[3-6]. The Se-Te alloys are found to be useful from the technological point of view if these alloys are thermally stable with time and temperature during use. However, thermal instability leading to crystallization is found to be one of the drawbacks of these alloys. Hence, attempts have been made to improve the stability of Se-Te binary alloys by the addition of third element. The insertion of an impurity in Se-Te binary alloy at the cost of Se is of interest owing to the advantages like higher glass transition temperature (T_g) and T_p and thermally more stable effects as compared to host Se-Te alloy[7,8]. Moreover, the insertion of a third element such as Pb affects the basic bonding. It is observed that the addition of the third element helps in getting cross linked structure thus increasing T_g and T_p of the binary alloy, improves the thermal stability, glass forming ability and reduces ageing effects[6-10]. Moreover, to know the chemical durability and glass forming ability of these types of materials is an important issue and in recent years, the intermediate phases have been identified in chalcogenide glasses. These phases represent glass composition where the glass-forming tendency is optimized and ideal stress-free networks exist[10]. In our previous study, on dielectric and AC conductivity measurements in Se-Te-Pb shows the significant impact on its conduction mechanism with the addition of Pb and it is observed that $Se_{79}Te_{20}Pb_1$ is a critical composition at which maxima occurs and the system becomes a chemically ordered alloy containing comparatively higher energy hetero-polar bonds[11]. The nano-crystalline lead chalcogenides have become prominent for variety of applications in solar cells, photo-detectors, field-effect transistors and as sensitive membrane materials for chemical sensors[12-14].

*Corresponding author (E-mail: bspatial@gmail.com)

Kinetics studies are always connected with the concept of activation energy and glass transition activation energy is associated with nucleation and growth process. This gives information relative to the stability and applicability of these materials. Crystallization kinetics plays an important role in determining the transport mechanisms, thermal stability and glass forming ability and thus eventually to determine the suitable range of operating temperature for a specific technological application before crystallization takes place. Differential scanning calorimetry (DSC) or differential thermal analysis (DTA) are the two common experimental techniques used for the thermal analysis due to the fact that they are easy to carry out, quite sensitive, require little sample preparation and relatively independent of the sample geometry. However, DSC is the most sensitive technique and measures the volume fraction transferred as a function of temperature and time by measuring the heat absorbed or liberated during the phase change. Furthermore, two methods namely isothermal and non-isothermal methods are used in crystalline studies. Under isothermal conditions, the sample is quickly heated to a temperature above the glass transition temperature and the heat evolved during the crystallization process at a constant temperature is recorded as a function of time. Therefore, in isothermal method it is impossible to reach a test temperature instantly and during a time, which system needs to stabilize, no measurements are possible[8]. So it is often difficult to carry out over a wide temperature range and seems to be a time consuming method. On the other hand, in non-isothermal method, the sample is heated from room temperature at a fixed heating rate and heat evolved is recorded as a function of time and temperature[6-8]. A chalcogen rich glass undergoes structural changes and crystallization when reheated in DSC or DTA experiment. In addition to exothermic crystallization peak, the DSC or DTA curve shows an endothermic peak corresponding to glass transition before crystallization. The kinetics of glass transition phenomenon is an important area in the study of semiconducting alloys. In chalcogenide glassy systems, the glasses exhibiting no exothermic crystallization reaction above T_g show a threshold switching and glasses having an exothermic crystallization reaction above T_g exhibiting memory type switching. Furthermore, the glass transition temperature represents the strength or rigidity of the glass structure in chalcogenide alloys. Since T_g of a particular glass also depends on its thermal history; its variation with heating rate is of sufficient importance for these materials.

In the present study, the overall amorphous − crystallization transformation kinetics of a-$Se_{79}Te_{20}Pb_1$ bulk alloy has been investigated under non-isothermal condition at three different heating rates (5, 10 and 15 °C/min). The apparent activation energy for glass transition and for crystallization region has been deduced using different empirical approaches. The kinetic exponent is deduced using Gao and Wang model. Glass forming ability and fragility has also been reported and discussed.

2 Experimental

Glassy sample of $Se_{79}Te_{20}Pb_1$ alloy is prepared using melt quenching technique. 5N highly pure (99.999%) materials are weighed with an accuracy of 10^{-4} g according to their atomic percentages and sealed in a quartz ampoule (length ~5 cm, diameter ~12 mm) under a vacuum of ~2×10^{-5} mbar. The sealed ampoule has been kept inside a furnace where the temperature is raised to 900 °C at a rate of 3-4 °C min^{-1}. The ampoule is rocked frequently for 10 h at maximum temperature to make the melt homogenous. The quenching of the melted sample is done in the ice cooled water very rapidly to prevent crystallization. The prepared bulk sample was crushed to a fine powder for further characterizations. The amorphous nature of the glassy alloy has been verified by x-ray diffraction (XRD)[11]. The thermal behaviour of the investigated glass is investigated using DSC. Approximately, 3-5 mg of sample in powder form is encapsulated in standard aluminium pan and heated at different heating rates from 5-15 °Cmin^{-1}. The values of glass transition temperature (T_g), the peak temperature of crystallization (T_p) and the melting temperature (T_m) were determined by using the microprocessor of the thermal analyser. The crystallized fraction (χ), at a given temperature, is given as $\chi = (A_T/A)$, where A is the total area of the exothermic peak between the onset temperature (T_i) where crystallization just begins and the temperature (T_f) where the crystallization is completed. A_T is the area between T_i and T. A best fit for the results is calculated by the least-squares fitting method for the activation energies and other kinetic parameters.

3 Results and Discussion

Figure 1 shows DSC thermogram recorded at heating rate 10°C/min for $Se_{79}Te_{20}Pb_1$ chalcogenide glass. Similar thermograms are also observed for other heating rates 5 and 15 °C/min (not shown here).

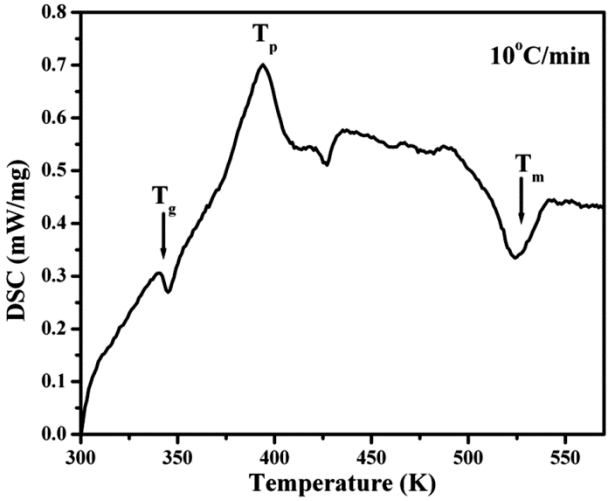

Fig. 1 – DSC thermogram of $Se_{79}Te_{20}Pb_1$ glass at heating rate 10 °C/min.

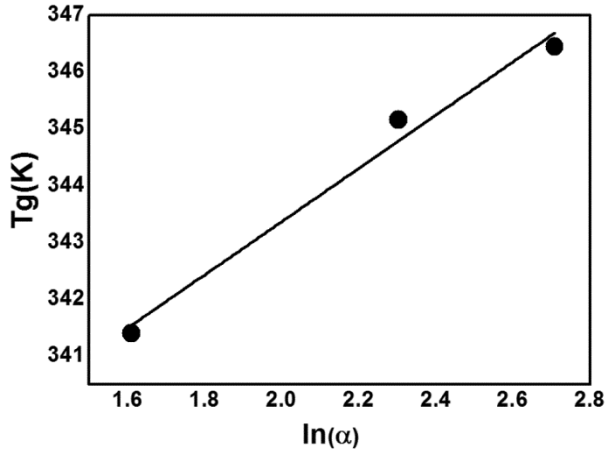

Fig. 2 – T_g versus ln(α) plot for $Se_{79}Te_{20}Pb_1$ chalcogenide glass.

The DSC trace of $Se_{79}Te_{20}Pb_1$ shows that the investigated sample exist in single glass transition and crystallisation phase. From these DSC thermograms, the investigated temperature region can be resolved into three typical characteristics. The first endothermic peak in DSC corresponds to the glass transition region; the exothermic peak corresponds to the crystallization and the last endothermic peak corresponds to the melting temperature. It is observed that T_g and T_p of the investigated alloy shift to the higher temperatures with the increase in heating rate. T_g is defined as the temperature at which the structural relaxation time becomes equal to the relaxation time of observation. The increase in T_g with heating rate is attributed to the relaxation dynamics in the glass transition period and varies inversely with the relaxation time[7]. Thus, the relaxation time of observation decreases with increasing heating rate and hence the glass transition temperature increases. The shift of T_p to the higher temperatures with increasing heating rate may be due to the fact that the system does not get sufficient time for nucleation and crystallization and by the time crystallization starts taking place, the temperature goes up with higher heating rates. The values of T_g, T_p and T_m at all heating rates are listed in table 1.

Table 1 — Parameter determined from heating rate data for $Se_{79}Te_{20}Pb_1$ chalcogenide glass.

Heating Rate	T_g	T_p	T_m	T_{rg}	K_{gl}	F_i
5	341.39	386.99	523.57	0.65	0.33	44.5
10	345.16	394.14	524.27	0.66	0.38	30.7
15	346.45	397.96	525.51	0.66	0.40	26.1

3.1 Glass transition activation energy

Glass transition activation energy is defined as the amount of energy which is absorbed by group of atoms in glassy region, so jump from one meta-stable state to other is possible and is involved in molecular motion and rearrangement of atoms around T_g. The glass transition temperature represents the strength or rigidity of the glass structure of the investigated glassy alloy. In present study, the glass transition region has been studied in terms of activation energy during glass transition and variation of glass transition temperature with heating rate. The glass transition temperature at different heating rate has been used to analyse the dependence of T_g on heating rate and estimate of the glass transition activation energy of $Se_{79}Te_{20}Pb_1$ bulk glass. Three approaches have been used to study the glass transition region. The first one corresponds to the empirical relation given by Lasocka[15]:

$$Tg = \mathrm{A} + \mathrm{B}in(\alpha) \quad \ldots (1)$$

where A and B are constants depending upon the glass composition. The plot between ln (α) and T_g should be a straight line and holds true for $Se_{79}Te_{20}Pb_1$ chalcogenide glass (Fig. 2). The constant A indicates the value of the glass transition temperature for heating rate of 1 $Kmin^{-1}$. The slope of B is related to cooling rate of the melt and lowers the cooling rate of melt, lower the value of B. Thus, the physical significance of B seems to be related with the response of the changes in the configuration within the glass transition region. The value of A and B are calculated from the intercept and slope and are found equal to (334 ± 1.33) K and (4.69 ± 0.6) min

respectively. It is found that this empirical relation holds very well for the present system.

The apparent glass transition activation energy E_g of the $Se_{79}Te_{20}Pb_1$ glassy alloy has been evaluated using Kissinger's formula[16]. Kissinger's equation is used to determine the activation energy of the crystallisation process. The reason of applying this method for the evaluation of the glass transition activation energy comes from the fact that shifting of the glass transition peak at different heating rates is similar to crystallisation peak. Kissinger's equation is given by:

$$ln\frac{\alpha}{Tg2} = -\frac{Eg}{RTg} + const. \quad \ldots (2)$$

where R is the universal gas constant. The variation of $\ln(\alpha/T_g^2)$ with $1/T_g$ should be a straight line. The slope of the plot gives the apparent glass transition activation energy (Fig. 3) and is found equal to (200.53 ± 3.2) kJmol^{-1}.

Other approach gives the heating rate dependence of the glass transition temperature in chalcogenide glasses which is interpreted by Moynihan *et al*[17] in term of thermal relaxation phenomenon. If variation of $1/T_g^2$ with $\ln(\alpha)$ is much slower than the variation of $1/T_g$ and $\ln(\alpha)$, the activation energy for the glass transition region E_g can be simplified and determined by relation:

$$\ln(\alpha) = -\frac{Eg}{RTg} + const. \quad \ldots (3)$$

Figure 4 shows the linear graph between $\ln(\alpha)$ versus $1000/T_g$ for three heating rates. The slope of the graph gives E_g and is found equal to (206.36 ± 3.2) kJmol^{-1}.

The activation of thermal relaxation (E_g) depends on the glass transition temperature (T_g), the heating rate α and the molecular motion and rearrangements of the atoms around T_g. The activation energy is equivalent to glass transition temperature and also depends on thermal history of its preparation. When sample is reheated again in a DSC furnace, the atom undergoes infrequent transition between the local potential minima separated by different energy barriers in the configurational space where each local minima represents different structure. The most stable local minima in the glassy region has lowest internal energy. The atoms in a glass having minimum activation energy have higher probability to jump to the meta-stable state of lower internal energy. Deduced values of glass transition activation energy from these two methods given above are in good accord with each other means any one approach can be used to calculate E_g.

3.2 Crystallisation activation energy

According to Kissinger's model, the effective crystallisation activation energy (E_c) can be determined from the variation of the peak crystallisation temperature (T_p) with heating rate α by using the following relation[15]:

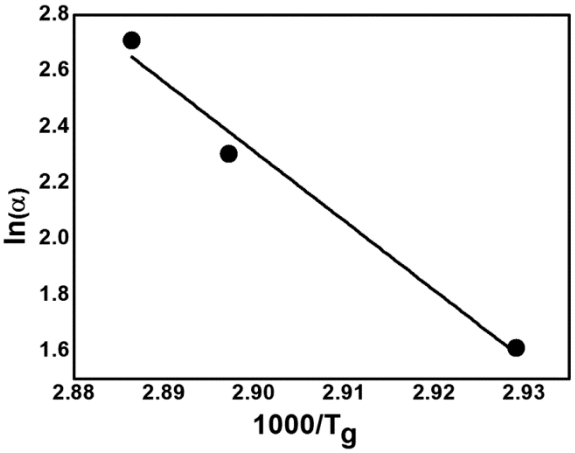

Fig. 4 – Plot of $\ln(\alpha)$ against $1000/T_g$ plot for $Se_{79}Te_{20}Pb_1$.

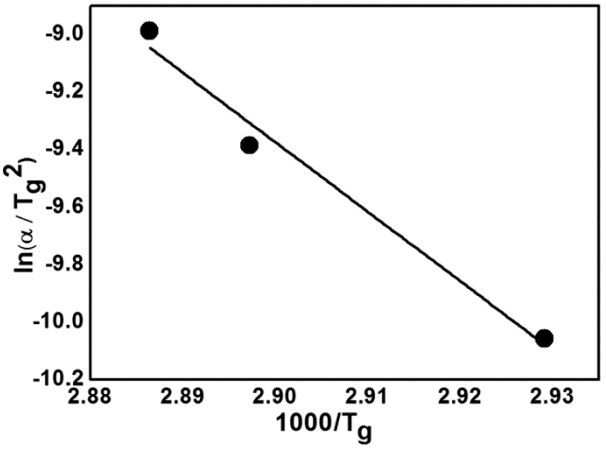

Fig. 3 – $\ln(\alpha/T_g^2)$ versus $1000/T_g$ plot for $Se_{79}Te_{20}Pb_1$.

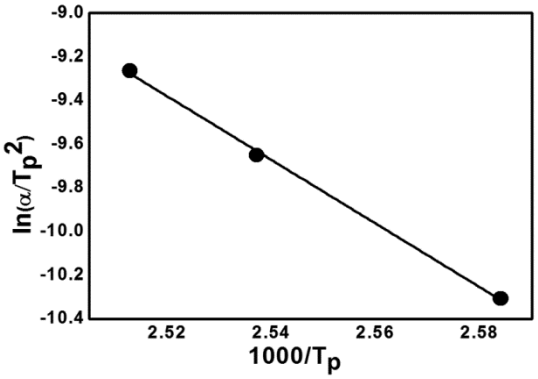

Fig. 5 – $\ln(\alpha/T_p^2)$ versus $1000/T_p$ plot for $Se_{79}Te_{20}Pb_1$.

$$\ln\left(\frac{\alpha}{Tp2}\right) = -\frac{Ec}{RTp} + const. \quad \ldots (4)$$

The slope of the plot between the $\ln(\alpha/T_p^2)$ versus $1/T_p$ (fig. 5) gives the value of the apparent crystallisation activation energy and the calculated value of E_c is found equal to 121.01 ± 0.47 kJmol^{-1}.

When the variation of $1/T_p^2$ with $\ln(\alpha)$ is much slower than the variation of $1/T_p$ with $\ln(\alpha)$, Mahadevan *et al*[18] gives above equation in the following form:

$$\ln(\alpha) = -\frac{Ec}{RTp} + const. \quad \ldots (5)$$

The apparent crystallisation activation energy can be determined from the slope of the plot of $\ln(\alpha)$ against $1/T_p$ shown in Fig. 6 and is found to equal to 127.53 ± 0.47 kJmol^{-1}.

The crystallisation activation energy can also be calculated using Augis-Bennett method[19]:

$$ln\left[\frac{\alpha}{(T_p - T_0)}\right] = -\frac{E_c}{RT_p} + lnk_0 \quad \ldots (6)$$

where T_o be the onset temperature for crystallisation. The application of method of Augis and Bennett involves the assessment of T_o that is dependent on the heating rate and accuracy of DSC or DTA curve fitting. Augis and Bennett[19] have suggested that a single value of T_o lower than the minimum onset temperature ($T_{o(\min)}$) to be used at all heating rates. Thus, according to Eq. (6) underlying the method of Augis and Bennett, a dependence of E_c on T_o is expected. On the other hand, the assumptions used for the derivation of Eq. (6) do not require the choice of the same value of T_o for all heating rates. The obtained values of E_c using $T_o = T_{onset}$ for each heating rate found from DSC curves were used and from the slope of the figure 7 function fitted to the data, the activation energy for the crystallisation process evaluated and was found equal to 121.24 ± 0.45 kJmol^{-1}. According to the value of the above equation the value of frequency factor is deduced from the intercept of the graph of $\ln(\alpha/T_p - T_o)$ versus $1/T_p$ and is found equal to (6.33×10^{15}) s^{-1}. By applying the method of Augis and Bennett considering $T_o = 0$ or in case of $T_p >> T_o$, the above equation can be approximated to following form 20:

$$ln\left(\frac{\alpha}{T_p}\right) = -\frac{E_c}{RT_p} + const. \quad \ldots (7)$$

The slope of Fig. 8 plotted for Eq. 7 gives the value of crystallisation activation energy and derived value is 124.27 ± 0.47 kJmol^{-1}.

The activation energy of crystallisation is calculated using different theoretical models. The crystallisation kinetics of amorphous alloys has been extensively studied using the classical Johnson-Mehl-Avrami (JMA) model for non-isothermal kinetics.

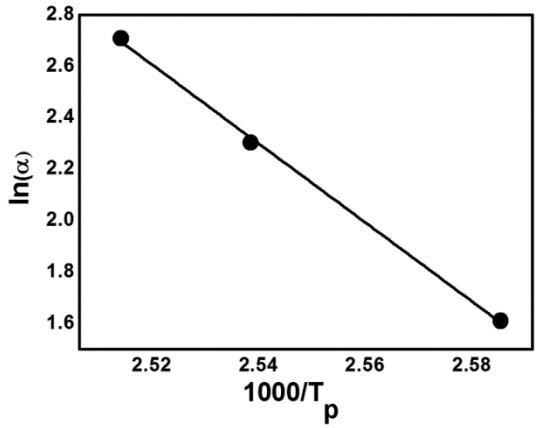

Fig. 6 – Plot of $\ln(\alpha)$ against $1000/T_p$ plot for chalcogenide $Se_{79}Te_{20}Pb_1$ glass.

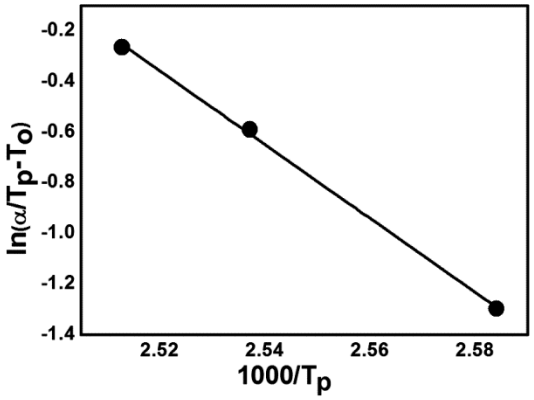

Fig. 7 – $\ln(\alpha/T_p - T_o)$ versus $1000/T_p$ for $Se_{79}Te_{20}Pb_1$.

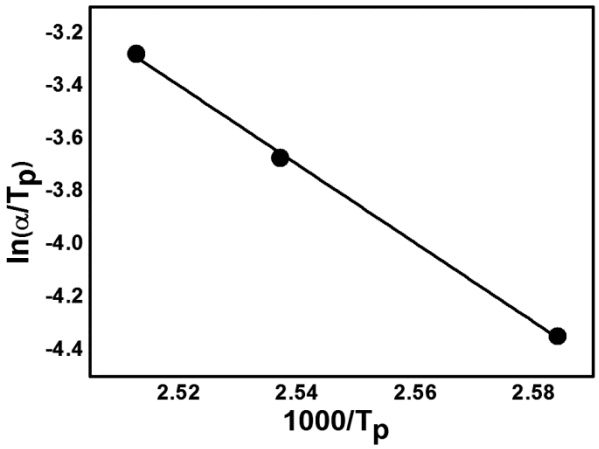

Fig. 8 – $\ln(\alpha/T_p)$ versus $1000/T_p$ for bulk $Se_{79}Te_{20}Pb_1$ alloy.

This model implies that the Avrami exponent (n) and the activation energy (E_c) should be constant during the transformation process. Generally the crystallisation process is well characterised when the three kinetic parameters, activation energy of crystallisation (E_c). Avrami exponent (n) and frequency factor (K_o) are determined.

Gao and Wang[21] proposed a slightly different method to analyse DSC curve in terms of activation energy (E_c), the dimensionality, rate constant in atomic diffusion, the frequency factor K_o etc during crystallisation process. The equation is also derived from JMA transformation equation and show the relationship between maximum crystallisation rate and the crystallisation peak temperature. Gao and Wang uses the following expression to determine activation energy:

$$\ln\left(\frac{d\chi}{dt}\right)_{T_p} = -\frac{E_c}{RT_p} + const. \quad \ldots (8)$$

Slope of above equation gives the value of E_c/R. Activation energy can be calculated by taking the variation of $\ln(d\chi/dt)_{Tp}$ against $1/T_p$. Slope of Fig. 9 gives the value of activation energy and is found equal to 120 ± 6.2 kJmol^{-1}. Moreover, this equation predicted that the maximum rate of crystallisation increases by the same factor as heating rate does in DSC. Figure 10 shows that the peak height increases and shift towards higher temperature value with increase in heating rate. This is due to the fact that as heating rate is increased from 5 to 15 °C/min, the rate of crystallisation increases and crystallisation shifts toward higher temperature. This may be interpreted as that with the increased rate of crystallisation, a greater volume fraction is crystallised in a smaller time as compared to the lower heating rate, which further signifies the increased peak height with increase in heating rate in these curves. The increase in $\ln(d\chi/dt)_{Tp}$ values as the heating rate does has also been discussed in literature[22,23].

The activation energy being an important parameter since it indicates the thermal stability of the glass and its magnitude reflects the nature of transformation. The values of crystallization activation energy obtained from different methods are nearly same and little difference can also be attributed to the fact that these models are based on approximations involved in obtaining the final equation of different formalisms.

3.3 Crystallisation reaction order (n)

The Gao and Wang model is also used to evaluate rate constant and Avrami exponent using equations as follows:

$$k = k_0\, exp\, \frac{E_c}{RT} \quad \ldots (9)$$

$$k_p = \frac{\alpha E_c}{RT_p^2} \quad \ldots (10)$$

$$\left(\frac{d\chi}{dt}\right)T_p = 0.37nk_p \quad \ldots (11)$$

where pre-exponential factor k_o is the frequency factor which gives the number of attempts per second made by nuclei to overcome the energy barrier which in turn gives information about the number of the nucleation sites. Avrami exponent n is calculated using Eq.11 and the average value of n is deduced equal to 2.03. Mahadevan *et al*[18] have shown that n may be 4, 3, 2, 1 which are related to different kinetic mechanisms n = 4, volume nucleation with three-dimensional growth;

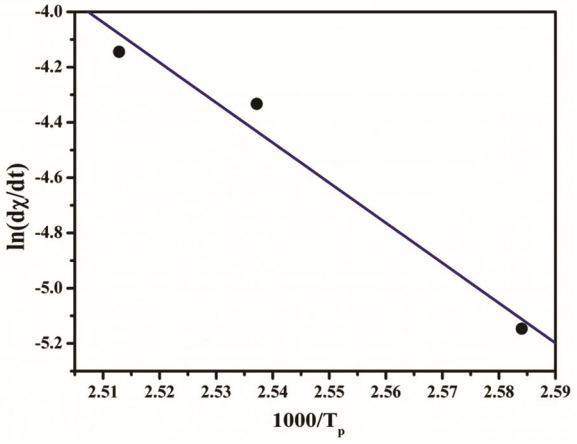

Fig. 9 – $\ln(d\chi/dt)$ versus $1000/T_p$ for $Se_{79}Te_{20}Pb_1$ glassy alloy.

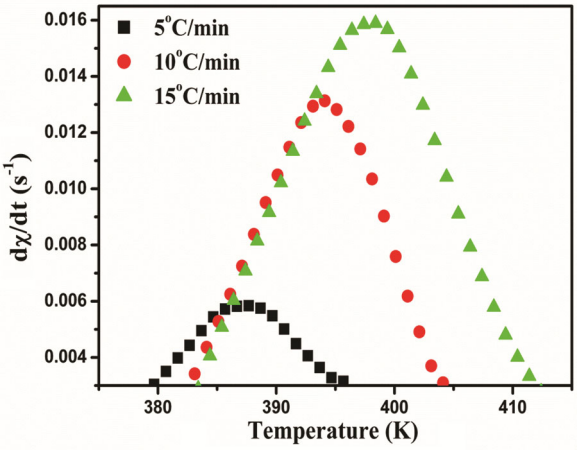

Fig. 10 – Crystallisation rate versus temperature of exothermic peak at three different heating rates

n = 3, volume nucleation with two-dimensional growth; n = 2, volume nucleation with one-dimensional growth; n = 1, surface nucleation with one-dimensional growth from surface to inside. The calculated value of n equals to 2.03 postulates a crystallisation mechanism for investigated alloy which shows predominantly one dimensional growth of $Se_{79}Te_{20}Pb_1$.

3.4 Thermal stability and the ease of glass formation

Thermal stability and the ease of glass formation are important factors to determine the various applications of the investigated glass. Kauzmann[24] gives a criterion of good glass forming ability (*GFA*) as reduced glass transition temperature, $T_{rg} \geq 2/3$. Glass forming ability (*GFA*) is determined by calculating the reduced glass transition temperature as:

$$T_{rg} = \frac{T_g}{T_m} \quad \ldots (12)$$

The composition obeying two-third rule ($T_{rg} \geq 0.65$) indicating the glass forming ability (*GFA*) for that composition of the material is high. The average value of T_{rg} of investigated composition is 0.65, showing that the glass forming ability of $Se_{79}Te_{20}Pb_1$ chalcogenide glass is high.

Thermal stability and *GFA* are important, for memory and switching material. ($T_p - T_g$) is strong indicator of both thermal stability and *GFA*. The higher the value of ($T_p - T_g$), higher is the thermal stability and *GFA*. The higher the value of this difference indicates more resistance to the crystallisation. The thermal stability and ease of glass formation may also be evaluated using Hruby's parameter[25]:

$$K_{gl} = \frac{(T_p - T_g)}{(T_m - T_p)} \quad \ldots (13)$$

Higher value of ($T_p - T_g$) delays the nucleation and the small value of ($T_m - T_p$) retards the growth process of nucleated crystals. Hruby's parameter combines the growth and nucleation aspect of the phase transformation. The value of K_{gl} varies from 0.33 to 0.40 and is listed in Table 1.

Since there is no absolute criterion to parameterise the glass formation, the empirical parameters used for its quantitative characterisation have been evaluated. The fragility index (F_i) is the important parameter of *GFA*. It is the measure of the rate at which the relaxation time decreases with increasing temperature around T_g and is given by[26,27]:

$$F_i = \frac{E_g}{RT_g ln(\alpha)} \quad \ldots (14)$$

According to Viglis[28], the glass-forming liquid that exhibit an approximate Arrhenian temperature dependence are defined as strong and specified with the low value of F_i ($F_i \approx 16$), while the limit of glass fragile glass-forming liquids is characterised by high value of F_i ($F_i \approx 200$). The values of F_i for all heating rate have been tabulated in Table 1 and indicate that the fragility index for present glass is 26.18−44.53, which is in the mentioned limit. However, F_i decreases with increasing heating rate and it may be ascribed due to the increase in T_g with heating rate. From the values of F_i we can say that glass obtain from good glass-forming liquid.

4 Conclusions

The glass transition phenomenon, amorphous-crystallisation transformation and the ease of glass formation of chalcogenide $Se_{79}Te_{20}Pb_1$ alloy have been studied. The kinetic parameters; namely glass transition activation energy, activation energy for crystallisation, kinetic exponent (n), reduced glass transition temperature, Hruby's parameter and fragility index have been deduced. Different empirical approaches have been used to evaluate the glass transition activation energy (E_g) and crystallisation activation energy (E_c). The crystallization mechanism is concluded to be one dimensional growth. Average activation energy for crystallisation process is found to be equal to 122.93 ± 2.95 kJmol^{-1}. The average value of glass transition activation energy is found equal to 203.45 ± 4.12 kJmol^{-1}. The reduced glass transition temperature (T_{rg}) and Fragility index (F_i) indicate that $Se_{79}Te_{20}Pb_1$ is made from good glass forming liquids.

References

1 Afify N, Hussein M A, EI-Kabany N & N Fathy N, *J Non-Cryst Solids*, 354 (2008) 3260.
2 Suri N, Bindra K S, Kumar P & Thangaraj R, *J Non-Cryst Solids*, 353 (2007) 1264.
3 Kasap S O & Juhasz C, *J Mater Sci*, 21 (1986) 1329.
4 Lucovsky G, Mooradian A,Taylor W, Wright G B & Keezer R C, *Solid State Commun*, 5 (1967) 113.
5 Schotmiller J, Tabak M, Lucovsky G & Ward A, *J Non-Cryst Solids*, 4 (1970) 80.
6 Patial B S, Thakur N & Triphati S K, *Phys Scripta*, 85 (2012) 045603.
7 Patial B S, Thakur N & Triphati S K, *Thermochim Acta*, 513 (2011) 1.
8 Patial B S, Thakur N & Triphati S K, *J Therm Anal Calorim*, 106 (2011) 845.

9 Yadav S, Srivastava S, Kumar D & Kumar A, *Indian J Pure Appl Phys*, 56 (2018) 884.
10 Ahmad M, Kumar P, Suri N, Kumar J & Thangaraj R, *Appl Phys A*, 94 (2009) 933.
11 Thakur A, Patial B S & Thakur N, *J Electron Mater*, 46 (2017) 1516.
12 Smith A W, *Appl Opt*, 13 (1974) 795.
13 Anjali, Patial B S, Bhardwaj S, Awasthi A M & Thakur N, *Physica B*, 523 (2017) 52.
14 Sharma N, Patial B S & Thakur N, *Indian J Pure Appl Phys*, 56 (2018) 128.
15 Lasocka M, *Mater Sci Eng*, 23 (1976) 173.
16 Kissinger H E, *J Res Nat Bur Stand,* 57 (1956) 217; *Anal Chem*, 29 (1957) 1702.
17 Moynihan C T, Easteal A J & Wilder J, *J Phys Chem*, 78 (1974) 2673.
18 Mahadevan S, Giridhar A & Singh A K *J Non-Cryst Solids*, 88 (1986) 11.
19 Augis J A & Bennett J E, *J Therm Anal*, 13 (1978) 283.
20 Yinnon H & Uhlmann D R, *J Non- Cryst Solids*, 54 (1983) 253.
21 Gao Y Q & Wang W, *J Non-Cryst Solids*, 81 (1986) 129.
22 Triphati S K, Patial B S & Thakur N, *J Therm Anal Calorim*, 107 (2012) 31.
23 Patial B S, Thakur N & Triphati S K, *J Nano-Electron Phys*, 5 (2013) 02017.
24 Kauzmann W, *Chem Rev*, 43 (1948) 219.
25 Hurby A, *Czech J Phys*, B22 (1972) 1187.
26 Mehta N, Tiwari R S & Kumar A, *Mater Res Bull*, 41 (2006) 1664.
27 Saffarini G, Saiter A, Garda M R & Saiter J M, *Physica B*, 389 (2007) 275.
28 Viglis T A, *Phys Rev B*, 47 (1993) 2882.